*RMxAC*, **58**, 16–18 (2024)

# WIND-BLOWN NEBULAE FROM MASSIVE STARS

J. Mackey[1]

RESUMEN

La interacción entre el viento estelar y el medio interestelar de una estrella que se mueve supersónicamente a través de este genera nebulosas de choque de proa. Simulaciones de esta interacción pueden modelar su emisión térmica desde radio hasta rayos X. Modelos hidrodinámicos axialmente simétricos predicen fuerte emisión difusa de rayos X en las turbulencias tras el paso del choque de proa, pero esta no se detecta en NGC 7635. Por el contrario, las simulaciones 3D con campos magnéticos predicen emisión difusa en rayos X inferior a la que se detecta en $\zeta$ Oph. Aquí presento un estudio preliminar de los efectos de resolución en el nivel de emisión en rayos X, demostrando que la emisión puede variar notablemente en tiempo y la necesidad de obtener cálculos de alta resolución para resolver las inestabilidades dinámicas en la discontinuidad de contacto.

ABSTRACT

Bow shocks are nebulae produced by interaction between stellar winds and the interstellar medium, when the star is moving supersonically through its surroundings. Simulations can model the interaction and its thermal emission from radio to X-rays. Axisymmetric hydrodynamic models predicted strong diffuse X-ray emission from the turbulent wake behind the star, but this was not detected in observations of NGC 7635. In contrast, 3D simulations including magnetic fields underpredicted the diffuse X-ray emission observed around $\zeta$ Oph. I present preliminary work studying the effects of resolution on the simulated X-ray emission, demonstrating significant time-variation in the emission and the importance of high-resolution calculations to resolve dynamical instabilities at the contact discontinuity.

*Key Words:* methods: numerical — ISM: bubbles — circumstellar matter — X-rays: ISM

## 1. INTRODUCTION

Nebulae are rare around main-sequence massive stars except for the runaway stars, where the dynamical pressure of the relative motion between star and interstellar medium (ISM) keeps the wind-ISM interaction region close to the star and also shock-compresses the interstellar gas (Henney & Arthur 2019a; Mackey 2023). The outer shock is typically isothermal so that large compression factors may occur. Because the whole region is photoionized by the central star's EUV radiation, this shocked ISM emits optical and infrared spectral lines of common diagnostic ions and bremsstrahlung in the radio band. Bow shocks also emit synchrotron radiation at radio wavelengths; see PhD project of M. Moutzouri and Moutzouri et al. (2022). Dust that is heated by the intense stellar radiation field emits brightly in the mid-infrared, and this is the most successful waveband for detecting bow shocks (van Buren & McCray 1988; Henney & Arthur 2019b). At the contact discontinuity between shocked ISM (with temperature $T \sim 10^4\,$K) and shocked stellar-wind ($T \sim 10^7\,$K) there is an interface layer of mixed material at intermediate temperatures, produced by hydrodynamic instabilities and subsequent turbulent mixing (Mackey et al. 2015; Toalá & Arthur 2018) and/or thermal conduction (Meyer et al. 2014). This gas may emit brightly in soft X-rays (Toalá et al. 2016, 2017) and UV lines (Boroson et al. 1997), depending on the effectiveness of the mixing processes.

Green et al. (2019) studied the Bubble Nebula (NGC 7635) using 2D hydrodynamical simulations assuming the nebula is produced by a runaway star moving into a dense ISM. These high-resolution simulations showed strong mixing at the wind-ISM interface, generated by shear-induced Kelvin-Helmholz instability (KHI), and resulting in a turbulent flow in the wake behind the star (similar to Mackey et al. 2015). Synthetic observations showed reasonable morphological agreement with infrared and optical emission from the nebula, but the predicted soft X-ray emission was significantly larger than the upper limits subsequently obtained by Toalá et al. (2020). The vigorous mixing in the simulated nebula was evidently stronger than is occuring in Nature.

To investigate this discrepency, Green et al. (2022) made 3D MHD simulations of the bow shock

[1]Dublin Institute for Advanced Studies, Astronomy & Astrophysics Section, DIAS Dunsink Observatory, Dublin, D15 XR2R, Ireland (jmackey@cp.dias.ie).

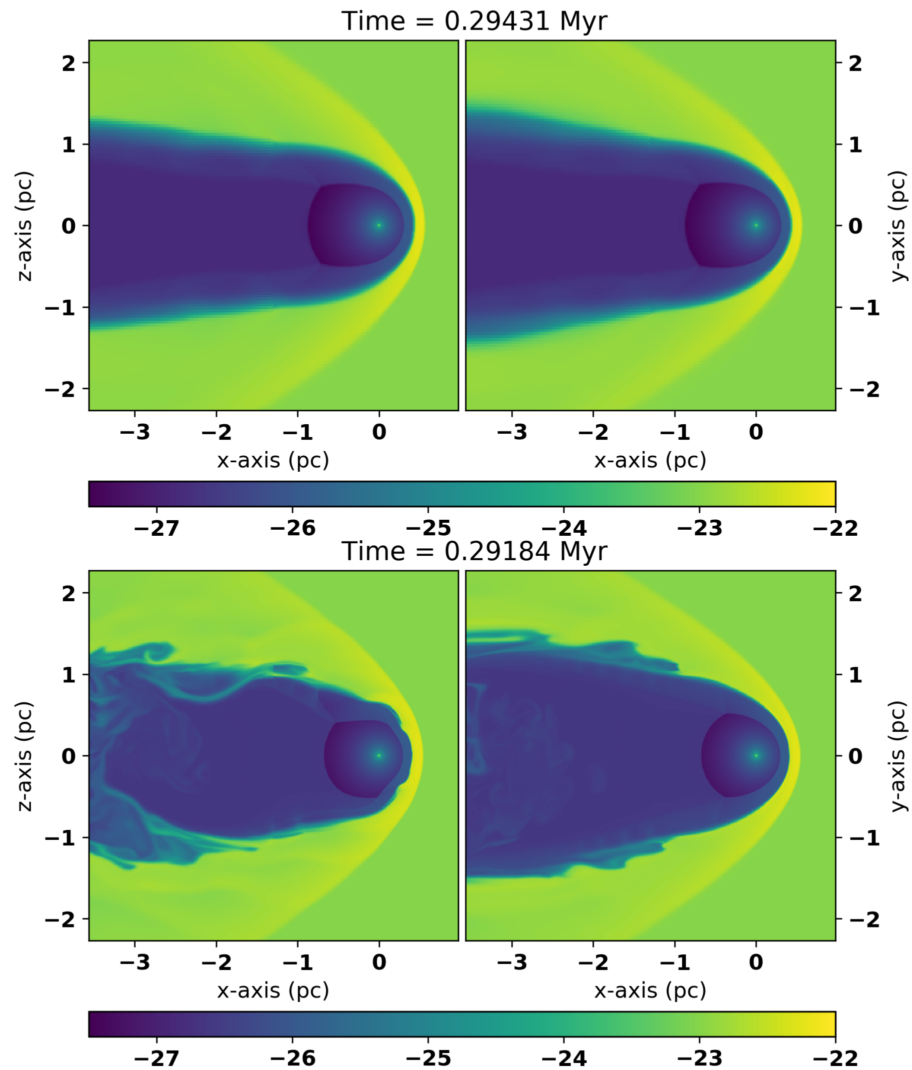


Fig. 1. Snapshots of $\log_{10}$ of gas density in $\mathrm{g\,cm^{-3}}$ from 3D simulations with low- ($128^3$, 3 refinement levels, above) and high- ($384^3$, 3 refinement levels, below) resolution, of the same bow shock using MHD with the ISM magnetic field almost perpendicular to the space velocity of the star. The star is moving from left to right into a uniform ISM and is located at the origin. In both plots the left panel shows the plane $y = 0$ and the right panel shows $z = 0$.

of $\zeta$ Oph, the closest O star to Earth and the only one with detected diffuse X-ray emission from the shocked stellar wind (Toalá et al. 2016). Surprisingly, they found that the simulations significantly *underpredicted* the soft X-ray emission compared with observations. This could have been a result of insufficient numerical resolution (the KHI was absent), suppression of mixing by magnetic fields, or because thermal conduction was not included in the calculations. This prompted us to undertake a study of the effects of different physical and numerical approximations on the resulting X-ray emission predicted by simulations, especially to assess numerical convergence. The same simulation was run with the PION MHD code (Mackey et al. 2021) in 2D and 3D, with (i) hydrodynamics and MHD, (ii) a diffusive (HLL) and a more accurate (HLLD) flux solver, and (iii) varying numerical resolutions consistent with available computing resources.

## 2. RESULTS

Simulations were run of the bow shock produced by a runaway star moving at $v_\star = 30\,\mathrm{km\,s^{-1}}$ in the positive $\hat{x}$ direction through a uniform ISM with density $\rho = 10^{-23}\,\mathrm{g\,cm^{-3}}$ and magnetic field $\mathbf{B} = \{1, 4, 0\}\,\mu\mathrm{G}$. Static mesh-refinement was used with 3 grid levels focused on the centre of the domain at the $+\hat{x}$ boundary, so that the apex of the bow shock

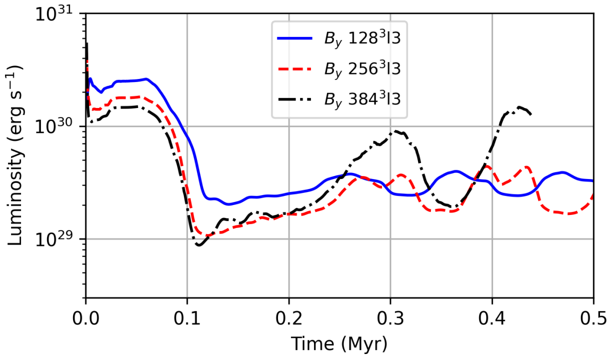


Fig. 2. X-ray emission (0.3–10 keV) from 3D MHD simulations of the same bow shock as a function of time for three different numerical resolutions.

has the highest spatial resolution. A reference frame is used such that the star is at rest with respect to the grid and located at the origin.

Slices through 3D MHD simulations plotting gas density on a logarithmic colour scale are shown in Figure 1. The upper panels show a low-resolution simulation with $128^3$ grid cells per level and 3 refinement levels. The lower panels show the same simulation but with $384^3$ grid cells per level and at an earlier time. Both simulations use the HLLD solver. The qualitative difference in the solution is obvious, with KHI active in the high-resolution case but not resolved in the low-resolution case. The KHI introduces some time-variation in the simulation properties for the high-resolution case, whereas the low-resolution simulation has reached an almost-stationary state.

Figure 2 shows predicted X-ray luminosity (0.3–10 keV) of the diffuse gas within the simulations as a function of time for three different resolutions as indicated in the legend. The dynamical timescale of the bow shock, $\tau \sim R_0/v_\star$ ($R_0$ is the distance from the star to the wind-termination shock), is approximately 0.1 Myr. The initial high X-ray emission followed by a sharp drop after 0.1 Myr is a relic of the initial conditions. At the lowest resolution the X-ray luminosity relaxes to an almost-constant value, reflecting the lack of KHI and the resulting time-variation that this process produces. At medium resolution ($256^3$ cells) there is more variation, about a factor of 3 from peak to trough, and at the highest resolution ($384^3$ cells) the variabiliity is an order of magnitude from peak to trough, driven by KHI. While this sequence of simulations has not converged numerically, the large range of X-ray luminosities found in the highest-resolution simulation is comparable to the range found for even higher-resolution 2D simulations.

## 3. CONCLUSIONS

A large suite of hydrodynamic and MHD simulations of bow shocks has been run and is currently being analysed (Mackey et al., in preparation). The preliminary results indicate that low-resolution 3D simulations may lack the spatial resolution to capture the KHI at the wind-ISM interface, resulting in a bow shock that is artificially stabilised by numerical diffusion. Higher-resolution simulations capture the KHI and the consequent turbulent mixing of wind and ISM material in the wake behind the star, resulting in time-variable X-ray emission that may vary by an order of magnitude depending on the time of observation. Using a turbulent model for the ISM (rather than the uniform medium considered here) may result in even stronger time variation.

**Acknowledgements:** I would like to thank my many colleagues who worked with me on these projects over the past 10 years; it has been a pleasure working with you all! This work was supported by a Royal Society-Science Foundation Ireland University Research Fellowship.

## REFERENCES

Boroson, B., McCray, R., Oelfke Clark, C., et al. 1997, ApJ, 478, 638
Green, S., Mackey, J., Haworth, T. J., Gvaramadze, V. V., & Duffy, P. 2019, A&A, 625, A4
Green, S., Mackey, J., Kavanagh, P., et al. 2022, A&A, 665, A35
Henney, W. J. & Arthur, S. J. 2019a, MNRAS, 486, 3423
———. 2019b, MNRAS, 489, 2142
Mackey, J. Winds of Stars and Exoplanets, ed. , A. A. VidottoL. Fossati & J. S. Vink, Vol. 370, 205–216
Mackey, J., Green, S., Moutzouri, M., et al. 2021, MNRAS, 504, 983
Mackey, J., Gvaramadze, V. V., Mohamed, S., & Langer, N. 2015, A&A, 573, A10
Meyer, D. M.-A., Mackey, J., Langer, N., et al. 2014, MNRAS, 444, 2754
Moutzouri, M., Mackey, J., Carrasco-González, C., et al. 2022, A&A, 663, A80
Toalá, J. A. & Arthur, S. J. 2018, MNRAS, 478, 1218
Toalá, J. A., Guerrero, M. A., Todt, H., et al. 2020, MNRAS, 495, 3041
Toalá, J. A., Marston, A. P., Guerrero, M. A., Chu, Y. H., & Gruendl, R. A. 2017, ApJ, 846, 76
Toalá, J. A., Oskinova, L. M., González-Galán, A., et al. 2016, ApJ, 821, 79
van Buren, D. & McCray, R. 1988, ApJ, 329, L93